

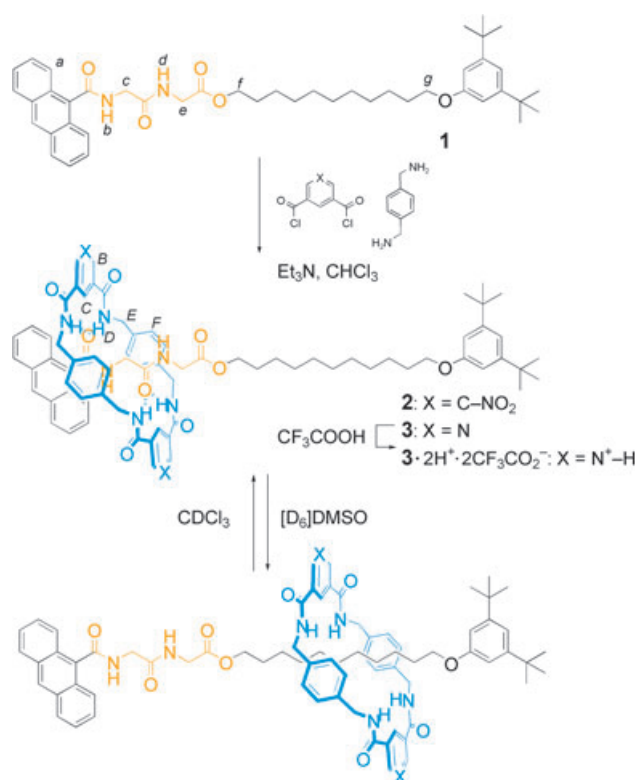
Patterning through Controlled Submolecular Motion: Rotaxane-Based Switches and Logic Gates that Function in Solution and Polymer Films**

David A. Leigh,* M. Ángeles F. Morales, Emilio M. Pérez, Jenny K. Y. Wong, Carlos G. Saiz, Alexandra M. Z. Slawin,* Adrian J. Carmichael, David M. Haddleton,* A. Manfred Brouwer,* Wybren Jan Buma,* George W. H. Worpel, Salvador León, and Francesco Zerbetto*

The extensive use of molecular machine-like processes in biology^[1] is inspiring efforts to exploit similarly well-controlled motions in functional synthetic systems.^[2] Stimuli-responsive “molecular shuttles”—rotaxanes in which a key feature of the tertiary structure, the relative positions of the interlocked components, can be changed in response to an external input—constitute a basic kind of nanoscale mechanical switch,^[3] capable of varying physical properties such as conductivity,^[4] circular dichroism,^[5] and fluorescence.^[6] However, there are few examples^[7] where shuttling has been demonstrated in the polymer-based media upon which many materials applications may ultimately depend, and only simple rotaxanes (not switchable molecular shuttles) have been used to create information-rich quaternary structures,

such as patterned surfaces.^[8] Here we report a system in which the translocation of a ring along a peptide-based thread, induced by changes in the nature of the local environment, can be used to switch the fluorescence of a rotaxane “on” or “off”. Remarkably, the system not only works in solution but also in polymer films where patterns visible to the naked eye can be generated solely through controlled submolecular motion. A polymer film “INHIBIT” logic gate based on a combination of control of submolecular positioning and chemical modification (protonation) is also demonstrated.

Thread **1** consists of an anthracene fluorophore (which also acts as a “stopper”) attached to a glycylglycine hydrogen-bonding binding site or “station”, which, in turn, is connected to a C₁₁ alkyl chain that can act as a second “solvophobic” station^[9] and is terminated by a second stopper.^[10] Rotaxanes **2** and **3** were prepared in 37 and 20% yields, respectively, by condensing *p*-xylenediamine with the appropriate bis(acid chlorides) in the presence of **1** (Scheme 1).^[11] Double proto-



Scheme 1. Synthesis and translational isomerism exhibited by environment-switchable molecular shuttles **2**, **3**, and $3 \cdot 2\text{H}^+ \cdot 2\text{CF}_3\text{CO}_2^-$.

nation of **3** with an excess of trifluoroacetic acid generated $3 \cdot 2\text{H}^+ \cdot 2\text{CF}_3\text{CO}_2^-$. The macrocycles in **2** and $3 \cdot 2\text{H}^+$ contain nitrophenyl and pyridinium moieties, respectively, which are known to quench the fluorescence of anthracene through distance-dependent electron transfer.^[6a,12]

A clear change in position of the rotaxane components of **2**, **3**, and $3 \cdot 2\text{H}^+ \cdot 2\text{CF}_3\text{CO}_2^-$ between CDCl_3 and $[\text{D}_6]\text{DMSO}$ (dimethylsulfoxide) is clearly apparent from ¹H NMR spectroscopy. Figure 1 shows the partial ¹H NMR spectra (400 MHz, 298 K) of thread **1** and rotaxane **2** in the different

[*] Prof. D. A. Leigh, Dr. M. Á. F. Morales, E. M. Pérez, Dr. J. K. Y. Wong
School of Chemistry, University of Edinburgh
The King's Buildings, West Mains Road, Edinburgh EH9 3J (UK)
Fax: (+44) 131-667-9085
E-mail: david.leigh@ed.ac.uk

Dr. C. G. Saiz, Prof. A. M. Z. Slawin
School of Chemistry, University of St. Andrews
Purdie Building, St. Andrews, Fife KY16 9ST (UK)
Fax: (+44) 1334-463-384
E-mail: amzs@st-and.ac.uk

Dr. A. J. Carmichael, Prof. D. M. Haddleton
Department of Chemistry, University of Warwick
Coventry CV4 7AL (UK)
Fax: (+44) 2476-524-112
E-mail: d.m.haddleton@warwick.ac.uk

Dr. A. M. Brouwer, Prof. W. J. Buma, Dr. G. W. H. Worpel
Institute for Molecular Chemistry, University of Amsterdam
Nieuwe Achtergracht 129, 1018 WS Amsterdam (The Netherlands)
Fax: (+31) 20-525-5670
E-mail: fred@science.uva.nl
wybren@science.uva.nl

Dr. S. León, Prof. F. Zerbetto
Dipartimento di Chimica “G. Ciamician”
Università degli Studi di Bologna
via F. Selmi 2, 40126 Bologna (Italy)
Fax: (+39) 051-209-9456
E-mail: francesco.zerbetto@unibo.it

[**] We thank C. A. Hunter for generating the FGIP for formamide. This work was supported by the European Union.

Supporting information for this article is available on the WWW under <http://www.angewandte.org> or from the author.

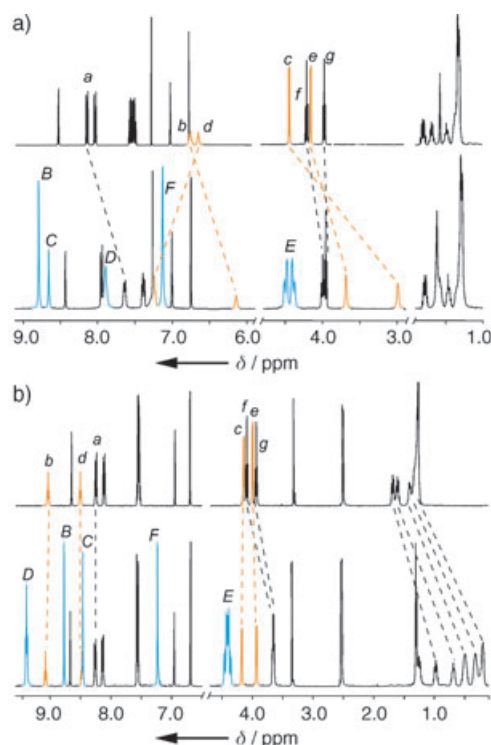


Figure 1. Partial ^1H NMR spectra of a) thread **1** (top) and rotaxane **2** (bottom) in CDCl_3 , and b) thread **1** (top) and rotaxane **2** (bottom) in $[\text{D}_6]\text{DMSO}$. The assignments correspond to the lettering shown in Scheme 1 and are based on COSY and GOESY experiments (400 MHz, 298 K). In CDCl_3 , the signals for H_c and H_e of the glycylglycine station (orange) are shielded by $\delta = 1.2$ and 0.4 ppm in the rotaxane with respect to the thread because of the aromatic rings of the macrocycle. In $[\text{D}_6]\text{DMSO}$, it is the signals that correspond to the protons of the alkyl chain that are strongly shielded, while the signals of the glycylglycine unit are essentially unchanged, which confirms the position of the macrocycle over the alkyl chain.

solvents. In CDCl_3 (Figure 1a) the chemical shift differences of the glycylglycine protons between **1** and **2** indicate that the macrocycle resides principally over the peptide residue of the rotaxane.^[13] The solid-state structure of a close analogue of **3** (only the non-anthracene stopper is different in **3'**) shows the macrocycle binding to the glycylglycine station through a network of intercomponent hydrogen bonds (Figure 2).^[14] In contrast, in $[\text{D}_6]\text{DMSO}$ (Figure 1b) it is the signals for the protons of the alkyl chains of **2** that are shielded by up to 1.2 ppm through encapsulation by the macrocycle. The discrimination of the macrocycle for the different regions of the thread is less well expressed in solvents of polarity and hydrogen-bonding basicity that lie in-between those of CDCl_3 and $[\text{D}_6]\text{DMSO}$ (e.g. $[\text{D}_3]\text{MeCN}$, $[\text{D}_4]\text{MeOH}$, $[\text{D}_8]\text{EtOAc}$, $[\text{D}_7]\text{DMF}$ ($\text{DMF} = N,N\text{-dimethylformamide}$), $[\text{D}_8]\text{THF}$ etc.), with smaller shifts involving more thread protons observed in the ^1H NMR spectra in these solvents than with CDCl_3 or $[\text{D}_6]\text{DMSO}$. However, the switching of the preferred translational isomer between the relatively nonpolar solvents and $[\text{D}_6]\text{DMSO}$ is quite general for rotaxanes with this type of amphiphilic thread, with **3** and $3\cdot 2\text{H}^+\cdot 2\text{CF}_3\text{CO}_2^-$ exhibiting similar shift patterns to **2** (see Supporting Information).

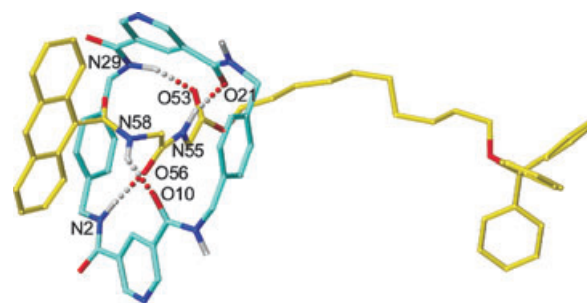


Figure 2. X-ray crystal structure^[14] of **3'**, a close structural analogue of rotaxane **3** (the 3,5-di-*tert*-butylphenyl stopper in **3** is substituted for a triphenylmethyl group to give **3'**). C (macrocycle) blue, C (thread) yellow, O red, N dark blue, H white. Non-amide hydrogen atoms are omitted for clarity. Intramolecular hydrogen-bond lengths [Å] and angles [°]: N2H–O56 1.93–170.7; N58H–O10 2.16, 140.6; N55H–O21 1.96, 174.4; N29H–O53 2.03, 161.9.

The effect of the environment-induced positional change of the interlocked components on the fluorescence emission of the rotaxanes was also investigated. Fluorescence spectra ($\lambda_{\text{ex}} = 340$ nm) of 10^{-5} M solutions of rotaxanes **2** and $3\cdot 2\text{H}^+\cdot 2\text{CF}_3\text{CO}_2^-$ were recorded in benzene, CH_2Cl_2 , CH_3CN , CH_3OH , DMF, DMSO, and H_2NCHO (Figure 3, Table 1). The variation in the ^1H NMR and fluorescence

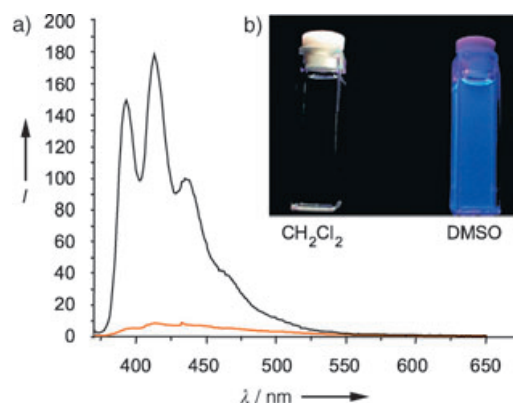


Figure 3. a) Fluorescence spectra ($\lambda_{\text{ex}} = 340$ nm, 1×10^{-5} M, 298 K) of rotaxane **2** in CH_2Cl_2 (orange) and DMSO (black). b) Photograph of the cuvettes that contain the solutions of rotaxane **2** illuminated at 254–350 nm which illustrate that the difference in fluorescence is clearly visible to the naked eye.

Table 1: Fluorescence quantum yields (φ_f) of rotaxanes **2** and $3\cdot 2\text{H}^+\cdot 2\text{CF}_3\text{CO}_2^-$ in various solvents, together with the dielectric constants (ϵ) and hydrogen-bond-donating (α_s)^[15] and -accepting (β_s)^[15] constants of the solvents.

| Solvent | ϵ | α_s | β_s | φ_f (2) | φ_f ($3\cdot 2\text{H}^+\cdot 2\text{CF}_3\text{CO}_2^-$) |
|--------------------------|------------|--------------------|--------------------|--------------------------|---|
| benzene | 2.3 | 1.0 | 2.2 | 0.004 | 0.003 |
| CH_2Cl_2 | 9.0 | 1.9 | 1.1 | 0.003 | 0.004 |
| CH_3CN | 37.5 | 1.7 | 4.7 | 0.003 | 0.004 |
| DMF | 37.0 | 1.6 | 8.3 | 0.013 | 0.007 |
| CH_3OH | 32.7 | 2.7 | 5.8 | 0.005 | 0.008 |
| DMSO | 49.7 | 0.8 | 8.9 | 0.032 | 0.019 |
| H_2NCHO | 109.5 | 2.9 ^[a] | 8.3 ^[a] | 0.029 | 0.042 |

[a] General values for the amide functional group.

spectra does not directly follow from the dielectric or hydrogen-bonding constants of the solvents, but is readily explained by considering the functional group interaction profiles (FGIP) recently introduced by Hunter (Figure 4).^[15] In solvents in which the intercomponent hydrogen bonding should be strongest (benzene, CH_2Cl_2 , CH_3CN) the anthracene fluorescence is virtually completely quenched, whereas in solvents with a strong solvophobic profile for alkyl chains

(DMSO and NH_2CHO), UV-stimulated fluorescence is clearly visible at submicromolar concentrations. This contrasts with the trend whereby an increase in dielectric constant generally increases the efficiency of other decay pathways to result in a decrease in fluorescence intensity.^[16] In fact, the very efficient quenching observed in nonpolar solvents suggests that the electron-transfer process in rotaxanes **2** and **3**· 2H^+ is close to the Marcus optimal region, where

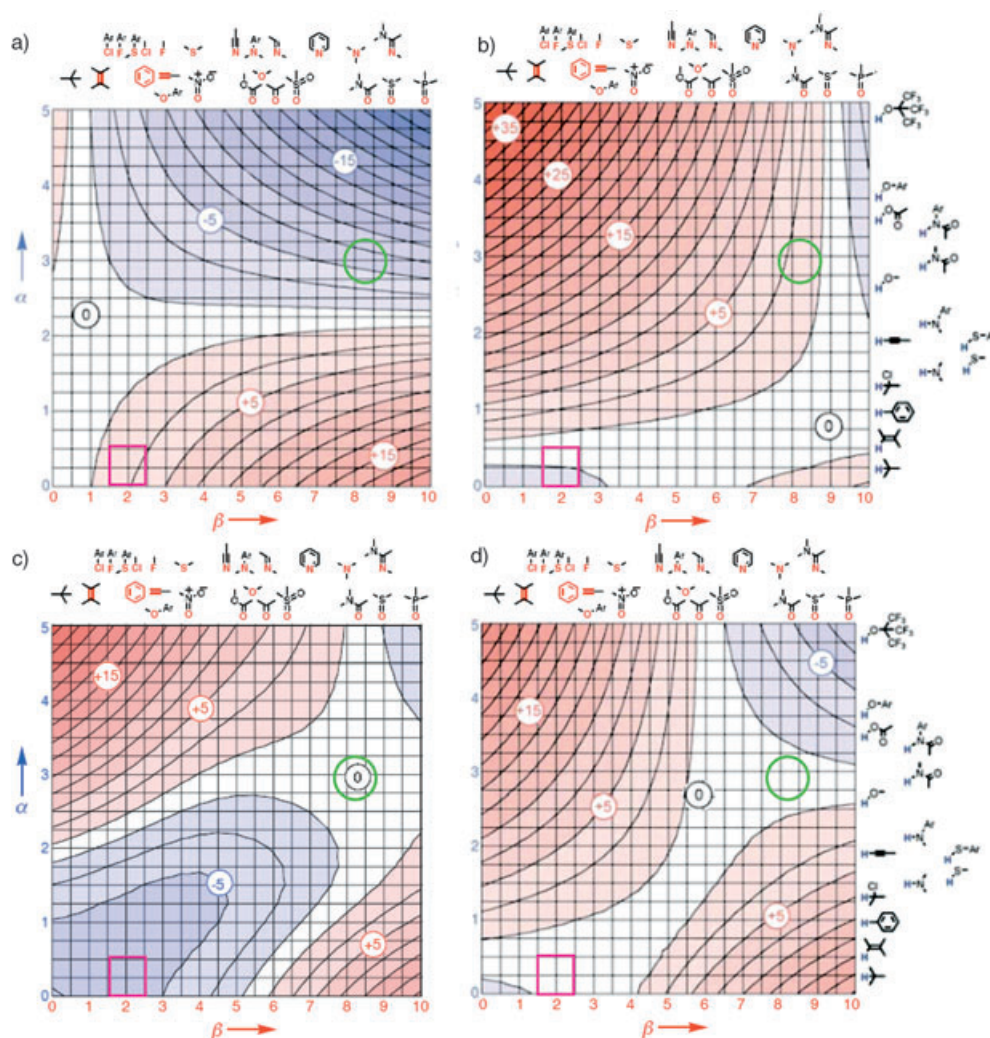
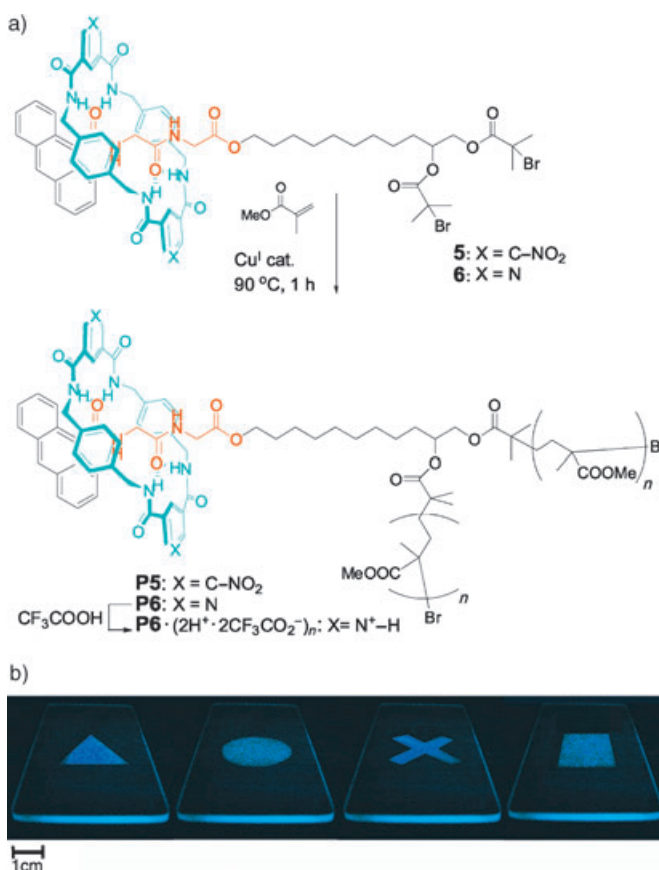


Figure 4. Functional group interaction profiles (FGIP) in a) chloroform ($\alpha_s=2.2$, $\beta_s=0.8$), b) DMSO ($\alpha_s=0.8$, $\beta_s=8.9$), c) formamide ($\alpha_s=2.9$, $\beta_s=8.3$),^[18] and d) methanol ($\alpha_s=0.9$ and 2.7 , $\beta_s=5.8$). Note, the FGIP of dichloromethane ($\alpha_s=1.9$, $\beta_s=1.1$) is very similar to that of chloroform. Blue represents a favorable interaction, and red represents an unfavorable interaction. Parts (a), (b), and (d) are reproduced with permission from Ref. [15]. The intercomponent interactions that largely determine the position and positional integrity of the macrocycle in **2**, **3**, and **3**· 2H^+ · $2\text{CF}_3\text{CO}_2^-$ are the amide–amide interaction region (highlighted with a green circle and corresponds to the peptidyl translational isomer) and the alkyl chain–phenyl ring interaction region (highlighted with a magenta square and stabilizes the alkyl translational isomer). a) Solute–solute amide–amide interactions are strongly favored and alkyl chain–phenyl ring interactions are disfavored, so we can expect the tertiary structure for the peptide-based molecular shuttles to feature the macrocycle held firmly on the peptide station by a well-defined hydrogen-bonding network, which leads to strong quenching of the anthracene fluorescence. b) Amide–amide interactions are strongly disfavored whereas alkyl chain–phenyl ring interactions in the solvent–solvent interaction dominated quadrant (bottom left) are favored, so we can expect the macrocycle to be localized on the alkyl-chain station but in a variety of positions and co-conformations owing to the general solvophobic interactions. As formamide contains both strong hydrogen-bond donors and acceptors it should display a strong solvophobic interaction in the lower left quadrant, similar to that for water. Indeed, this is the case as shown in (c), and the FGIP indicates that the solvophobic effect in NH_2CHO should be at least as strong as in DMSO, as suggested by the fluorescence measurements. d) In methanol, the amide–amide interactions are weak, but no driving force exists for alkyl-chain–phenyl-ring interactions either. So we can expect the room-temperature Boltzmann-averaged distribution to feature the macrocycle spending a significant amount of time over many positions along the entire length of the rotaxane thread; some of these conformations will lead to efficient quenching, while others do not.

the reorganization energy is equal to the $-\Delta G$ value for electron transfer (this inference is also supported by low-temperature fluorescence spectra and thermodynamic considerations, see Supporting Information). In such circumstances the electron-transfer process is barrierless and is insensitive to the polarity of the solvent.^[17] We can thus conclude that the variations in intensity observed with the different solvents is caused by the change in the relative separation of the fluorophore and quencher. Although the positioning of the macrocycle on the large alkyl-chain region would be expected to be rather poorly defined through a solvophobic effect, the ratio of fluorescence quantum yields obtained solely by the average net displacement of the macrocycle along the thread is as high as 15:1 (Table 1). This is significantly less than the 200:1 on/off ratio reported recently^[6a] for a light-switchable shuttle with two discrete and well-separated hydrogen-bonding stations, but is nonetheless remarkable for such a simple system and easily visible to the naked eye (Figure 3b).

To see if the same principles could be demonstrated to work in environments that are more relevant to materials applications, we synthesized well-defined polymer analogues of **2** and **3** by transition-metal-mediated living radical polymerization (often called ATRP)^[19] using methyl methacrylate as a monomer and [2]rotaxanes **5** and **6** as initiators. The resulting poly(methyl methacrylate) (PMMA)-based macromolecule [2]rotaxanes **P5** and **P6** had narrow polydispersity indices (PDI) of 1.17 and 1.14, respectively, and contained approximately 10% w/w of peptide rotaxane end-groups. ¹H NMR studies in CDCl₃ and [D₆]DMSO showed that the translational isomerism of the interlocked components of polymers **P5** and **P6** in solution exactly mirrored those of the small-molecule analogues, **2** and **3**. Thin transparent films of **P5** and **P6** on quartz slides were prepared through either conventional spin-coating techniques or by the evaporation of solutions of the polymers in dichloromethane. The resulting colorless thin films were of good optical quality and behaved in a manner independent of their method of preparation.

No fluorescence was detected when slides coated with the **P5** film were illuminated with UV light (254–350 nm), which suggests that in the nonpolar environment of the PMMA-like film the macrocycle resides over the peptide portion of the thread and efficiently quenches the anthracene fluorescence. However, although exposing the **P5**-coated slides to DMSO vapor (generated by gently warming an open beaker of the solvent in the vicinity of the film for 5 min) did not result in a noticeable change to the film under natural light, upon illumination with the UV source the characteristic blue anthracene fluorescence became apparent. Masking regions of films of **P5** from DMSO vapor with aluminum grids again produced no perceptible change under natural light, but distinctly shaped and clearly visible patterns were revealed with the UV source (Scheme 2b). The system is reversible: warming the slides to 70 °C at 0.1 Torr for 15 minutes to drive off absorbed solvent resulted in the loss of the fluorescent patterning. The behavior of **P5** implies that the environment-induced change in position of the interlocked components occurs in the polymer film just as it does in solution. This view



Scheme 2. a) Chemical structures of rotaxane initiators **5** and **6** and the corresponding PMMA-based polymers **P5**, **P6**, and **P6·(2H⁺·2CF₃CO₂⁻)_n**. b) Images obtained by casting films of polymer **P5** on quartz slides, then covering the films with aluminum masks, and exposing the unmasked area to DMSO vapor for 5 minutes. The photographs were taken while illuminating the slides with an 8-watt Camag UV lamp (254–350 nm) and reveal representative triangle, circle, cross, and square symbols.

is supported by molecular dynamics simulations (see Supporting Information) in which close similarities are seen between the average intercomponent separation of **2** in CH₂Cl₂ and DMSO and **P5** in a solvent-free environment and with the addition of several molecules of DMSO.

The quartz slides coated with **P6** films were fluorescent when illuminated with UV light as the pyridine units of the macrocycle need to be protonated to quench the excited state of anthracene. Accordingly, when quartz slides coated with **P6** were exposed to CF₃CO₂H vapors (**P6** → **P6·(2H⁺·2CF₃CO₂⁻)_n**) fluorescence was no longer observed. Figure 5b shows a distinct pattern of dark (nonfluorescent) bands resulting from thin films of **P6** upon exposure to CF₃CO₂H vapor through a striped aluminum mask (Figure 5a) and then illuminated with UV light. When the resulting dark strips of **P6·(2H⁺·2CF₃CO₂⁻)_n** were exposed to DMSO vapor through the same mask rotated by 90°, a criss-cross pattern was produced (Figure 5c) in which only segments that had been exposed to CF₃CO₂H vapor but not to DMSO vapor were dark when illuminated with the UV source, which suggest that displacement of the macrocycle

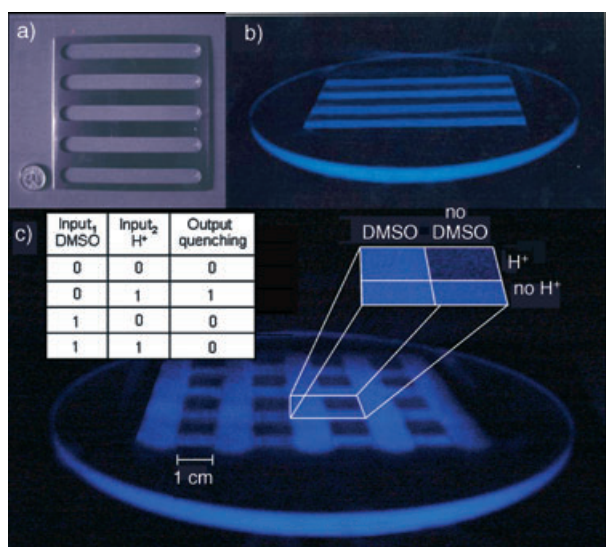


Figure 5. a) Aluminum grid used in the experiment; the coin shown for scale in the lower left corner of (a) is a UK 5 p piece. b) Pattern generated when films of **P6** were exposed to trifluoroacetic acid vapor for 5 minutes through the aluminum-grid mask. c) Criss-cross pattern obtained by rotation of the aluminum grid by 90° and exposure of the film shown in (b) to DMSO vapor for a further 5 minutes; only regions exposed to trifluoroacetic acid but not to DMSO are quenched, as shown in the magnified view. Inset: The truth table for an "INHIBIT" logic gate. The photographs of the slides were taken in the dark while illuminating with an 8-watt UV lamp (254–350 nm).

from the peptide station to the alkyl chain restores fluorescence to the exposed regions. The response of **P6** to the different combinations of two stimuli (DMSO and protons) corresponds to an "INHIBIT" Boolean logic gate.^[20,21] The **P6** logic gate does not operate with full reversibility as a film, however, because although the DMSO could be removed by warming under reduced pressure (as with **P5**), the effects of the acid stimulus could not be reversed without some deterioration in the optical quality of the film. In solution, **P6** is cleanly regenerated by treatment with base, for example, triethylamine.

In conclusion, we have described a class of molecular shuttles in which translational isomerism of the components can be controlled to either permit or preclude fluorescence quenching by intercomponent electron transfer in both solution and polymer films. As the shuttling mechanism does not require a change to the covalent structure of the shuttles, the optical response can be unambiguously ascribed to changes in the relative positions of macrocycle and thread; a visible optical response from a mechanical submolecular event.^[21] Although using exposure to chemical vapors as a stimulus is unlikely to be practically useful beyond sensing or, perhaps, security applications, related hydrogen-bonded shuttles can be switched in solution by using light,^[23] electrochemistry,^[24] changes in temperature^[25] or pH,^[26] and covalent-bond-forming chemical reactions.^[27] The present work demonstrates that some of the switching mechanisms, properties, and logic operations established for molecular shuttles in solution can be transferred to media that are more suitable for

developing materials which function through controlled submolecular motion.

Received: January 12, 2005

Published online: April 12, 2005

Keywords: fluorescence · logic gates · molecular devices · rotaxanes · solvent effects

- [1] M. Schliwa, *Molecular Motors*, Wiley-VCH, Weinheim, **2003**.
- [2] a) *Molecular Catenanes, Rotaxanes, and Knots: A Journey Through the World of Molecular Topology* (Eds.: J.-P. Sauvage, C. Dietrich-Buchecker), Wiley-VCH, Weinheim, **1999**; b) V. Balzani, A. Credi, F. M. Raymo, J. F. Stoddart, *Angew. Chem.* **2000**, *112*, 3484–3530; *Angew. Chem. Int. Ed.* **2000**, *39*, 3348–3391; c) V. Balzani, M. Venturi, A. Credi, *Molecular Devices and Machines—A Journey into the Nanoworld*, Wiley-VCH, Weinheim, **2003**; d) "Synthetic Molecular Machines": E. R. Kay, D. A. Leigh in *Functional Artificial Receptors* (Eds.: T. Schrader, A. D. Hamilton), Wiley-VCH, Weinheim, **2005**.
- [3] Most shuttling mechanisms require a concomitant—and often major—change in the rotaxane primary structure (e.g. charge, oxidation state, protonation, etc). In the absence of clear controls, attributing the changes in property to the positional displacement of components rather than the change in the electronic nature or chemical composition of the molecule is not straightforward.
- [4] a) A. H. Flood, R. J. A. Ramirez, W.-Q. Deng, R. P. Muller, W. A. Goddard, J. F. Stoddart, *Aust. J. Chem.* **2004**, *57*, 301–322; b) A. H. Flood, J. F. Stoddart, D. W. Steuerman, J. R. Heath, *Science* **2004**, *306*, 2055–2056.
- [5] G. Bottari, D. A. Leigh, E. M. Pérez, *J. Am. Chem. Soc.* **2003**, *125*, 13360–13361.
- [6] a) E. M. Pérez, D. T. F. Dryden, D. A. Leigh, G. Teobaldi, F. Zerbetto, *J. Am. Chem. Soc.* **2004**, *126*, 12210–12211; b) Q.-C. Wang, D.-H. Qu, J. Ren, K. Chen, H. Tian, *Angew. Chem.* **2004**, *116*, 2715–2719; *Angew. Chem. Int. Ed.* **2004**, *43*, 2661–2665; c) D.-H. Qu, Q.-C. Wang, J. Ren, H. Tian, *Org. Lett.* **2004**, *6*, 2085–2088.
- [7] a) D. W. Steuerman, H.-R. Tseng, A. J. Peters, A. H. Flood, J. O. Jeppesen, K. A. Nielsen, J. F. Stoddart, J. R. Heath, *Angew. Chem.* **2004**, *116*, 6648–6653; *Angew. Chem. Int. Ed.* **2004**, *43*, 6486–6491; b) A. H. Flood, A. J. Peters, S. A. Vignon, D. W. Steuerman, H.-R. Tseng, S. Kang, J. R. Heath, J. F. Stoddart, *Chem. Eur. J.* **2004**, *10*, 6558–6564.
- [8] M. Cavallini, F. Biscarini, S. León, F. Zerbetto, G. Bottari, D. A. Leigh, *Science* **2003**, *299*, 531.
- [9] a) A. S. Lane, D. A. Leigh, A. Murphy, *J. Am. Chem. Soc.* **1997**, *119*, 11092–11093; b) T. Da Ross, D. M. Guldi, A. Farran Morales, D. A. Leigh, M. Prato, R. Turco, *Org. Lett.* **2003**, *5*, 689–691; c) J. S. Hannam, S. M. Lacy, D. A. Leigh, C. G. Saiz, A. M. Z. Slawin, S. G. Stithell, *Angew. Chem.* **2004**, *116*, 3322–3326; *Angew. Chem. Int. Ed.* **2004**, *43*, 3260–3264; A solvent-switchable shuttle system has been developed for polyrotaxanes by Gibson and co-workers: d) C. Gong, H. W. Gibson, *Angew. Chem.* **1997**, *109*, 2426–2428; *Angew. Chem. Int. Ed. Engl.* **1997**, *36*, 2331–2333; e) C. Gong, T. E. Glass, H. W. Gibson, *Macromolecules* **1998**, *31*, 308–313; f) P. E. Mason, W. S. Bryant, H. W. Gibson, *Macromolecules* **1999**, *32*, 1559–1569.
- [10] G. W. H. Wurpel, A. M. Brouwer, I. H. M. van Stokkum, A. Farran, D. A. Leigh, *J. Am. Chem. Soc.* **2001**, *123*, 11327–11328.
- [11] D. A. Leigh, A. Murphy, J. P. Smart, A. M. Z. Slawin, *Angew. Chem.* **1997**, *109*, 752–756; *Angew. Chem. Int. Ed. Engl.* **1997**, *36*, 728–732.

- [12] J. H. Clements, S. E. Webber, *Macromolecules* **2004**, *37*, 1531–1536.
- [13] Several low-energy hydrogen-bonding motifs (secondary structure) of the peptide-based molecular shuttles are in equilibrium in nonpolar solvents.^[10] However, the relative position of the components (tertiary structure) is similar in each.
- [14] Crystal data for **3**: $C_{78}H_{76}N_8O_9$, $M_r = 1269.47$, clear crystal of dimensions $0.005 \times 0.02 \times 0.1 \text{ mm}^3$, monoclinic, $P2_1/n$ (no. 14); $a = 11.3523(3)$, $b = 35.6055(6)$, $c = 16.1772(3) \text{ \AA}$; $\beta = 95.3420(10)^\circ$, $V = 6510.5(2) \text{ \AA}^3$, $\rho_{\text{calcd}} = 1.295 \text{ Mg m}^{-3}$, $Z = 4$; synchrotron radiation (CLRC Daresbury Laboratory Station 9.8, silicon monochromator, $\lambda = 0.68740 \text{ \AA}$), $T = 160(2) \text{ K}$; 36465 reflections measured, 13843 unique. The structure was solved and refined on 881 variables, using the teXsan crystallographic package of the Molecular Structure Corporation to yield final residuals of $R = 0.215$ and $R_w = 0.332$. All hydrogen atoms on carbon atoms were placed in idealized fixed geometries. All hydrogen atoms on nitrogen atoms were located from a ΔF map and allowed to refine. CCDC-159773 contains the supplementary crystallographic data for this paper. These data can be obtained free of charge from the Cambridge Crystallographic Data Centre via www.ccdc.cam.ac.uk/data_request/cif.
- [15] C. A. Hunter *Angew. Chem.* **2004**, *116*, 5424–5439; *Angew. Chem. Int. Ed.* **2004**, *43*, 5310–5324.
- [16] A. P. de Silva, H. Q. N. Gunaratne, T. Gunnlaugsson, A. J. M. Huxley, C. P. McCoy, J. T. Rademacher, T. E. Rice, *Chem. Rev.* **1997**, *97*, 1515–1566.
- [17] J. Kroon, J. W. Verhoeven, M. N. Paddon-Row, A. M. Oliver, *Angew. Chem.* **1991**, *103*, 1398–1404; *Angew. Chem. Int. Ed. Engl.* **1991**, *30*, 1358–1361.
- [18] Generated by using equation 12 in Ref. [15] (C. A. Hunter, personal communication).
- [19] a) D. M. Haddleton, M. C. Crossman, B. H. Dana, D. J. Duncalf, A. M. Heming, D. Kukulj, A. J. Shooter, *Macromolecules* **1999**, *32*, 2110–2119; b) M. Kamigaito, T. Ando, M. Sawamoto, *Chem. Rev.* **2001**, *101*, 3689–3745; c) F. Lecolley, C. Waterson, A. J. Carmichael, G. Mantovani, S. Harrison, H. Chappell, A. Limer, P. Williams, K. Ohno, D. M. Haddleton, *J. Mater. Chem.* **2003**, *13*, 2689–2695.
- [20] For a recent review on molecular-scale logic gates, see: A. P. de Silva, N. D. McClenaghan, *Chem. Eur. J.* **2004**, *10*, 574–586.
- [21] For a polymer-based Boolean logic gate that operates in solution, see: S. Uchiyama, N. Kawai, A. P. de Silva, K. Iwai, *J. Am. Chem. Soc.* **2004**, *126*, 3032–3033.
- [22] R. A. van Delden, N. Koumura, N. Harada, B. L. Feringa, *Proc. Natl. Acad. Sci. USA* **2002**, *99*, 4945–4949.
- [23] a) A. M. Brouwer, C. Frochot, F. G. Gatti, D. A. Leigh, L. Mottier, F. Paolucci, S. Roffia, G. W. H. Wurpel, *Science* **2001**, *291*, 2124–2128; b) A. Altieri, G. Bottari, F. Dehez, D. A. Leigh, J. K. Y. Wong, F. Zerbetto, *Angew. Chem.* **2003**, *115*, 2398–2402; *Angew. Chem. Int. Ed.* **2003**, *42*, 2296–2300.
- [24] A. Altieri, F. G. Gatti, E. R. Kay, D. A. Leigh, F. Paolucci, A. M. Z. Slawin, J. K. Y. Wong, *J. Am. Chem. Soc.* **2003**, *125*, 8644–8654.
- [25] G. Bottari, F. Dehez, D. A. Leigh, P. J. Nash, E. M. Pérez, J. K. Y. Wong, F. Zerbetto, *Angew. Chem.* **2003**, *115*, 6066–6069; *Angew. Chem. Int. Ed.* **2003**, *42*, 5886–5889.
- [26] C. M. Keaveney, D. A. Leigh, *Angew. Chem.* **2004**, *116*, 1242–1244; *Angew. Chem. Int. Ed.* **2004**, *43*, 1222–1224.
- [27] D. A. Leigh, E. M. Pérez, *Chem. Commun.* **2004**, 2262–2263.